Green Chemistry

Accepted Manuscript

ROYAL SOCIETY OF CHEMISTRY

www.rsc.org/greenchem

Journal Name

RSCPublishing

ARTICLE

Magnetic nanohydrometallurgy: a nanotechnological approach to elemental sustainability

Henrique E. Toma

Cite this: DOI: 10.1039/x0xx00000x

Received 00th January 2012,
Accepted 00th January 2012

DOI: 10.1039/x0xx00000x

www.rsc.org/

Magnetic nanohydrometallurgy (MNHM), although yet in a very incipient stage, is opening new exciting perspectives in the conventional hydrometallurgy, aggregating nanotechnology to the mineral area. MNHM is based on the same principles of coordination chemistry successfully employed in modern extractive hydrometallurgy processes; however it uses specially designed superparamagnetic nanoparticles for capturing, transporting, confining and processing metal ions, with the aid of an external magnet. The working nanoparticles are completely recovered after the electrodeposition process, sustaining a cyclic process which can be automated, without using organic solvents and intensive chemical processing, as is the case of the current extractive hydrometallurgy and electrowinning technology. At the laboratory scale, the entire procedure can be performed in the same reactor, fulfilling, in addition to the processing and recovery facilities, the most important requisites of Green Chemistry.

Instituto de Química, Universidade de São Paulo, 05508-000, São Paulo, Brazil

E-mail: henetoma@iq.usp.br Fone 55 (11) 30913887

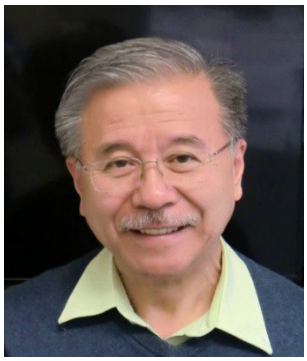

Henrique E. Toma is Professor of Chemistry at the University of São Paulo, Guggenheim Fellow, Member of the Brazilian Academy of Sciences and TWAS, and his major interests are Inorganic, Bioinorganic and Supramolecular Chemistry, Molecular Nanotechnology, and Green Nanotechnological strategies for Energy, Petroleum and Hydrometallurgy.

1. Introduction

Metals, as strategic materials, have dictated the most important changes in humanity evolution. Their knowledge and usefulness have opened new ages of development of mankind, providing better tools and materials for domestic use, agriculture and construction, as well as, supplying the power to the brave warriors in their past historical wars. Nowadays, even considering the great impact of the synthetic petrochemical and silicon materials, metals still remain a major partner in the human life.

Metal ores are widespread in nature, but their rational exploration and recycling are becoming increasingly important for the sustainable industrial development encompassing the demands of the economy, environment and society.[1,2] This is a rather complex subject. Besides the scientific and technological aspects, the richness brought by the exploration of mineral resources has also been a source of problems, from the unbalanced distribution to the people, to the deleterious effects on the environment. In addition, humanity should be prepared to deal with the inevitable depletion of ores displaying high metal content. New strategies are demanded by the mineral sector, which remains at the top position in the rank of pollution and environmental concerns. A great investment should be applied by the developing countries to surpass their status of commodity producers,

by rationally exploring their richness and aggregating more technology in the benefit of the society.

Extracting metals from ores involves a number of mechanical and chemical operations known as extractive metallurgy.[3-10] Pyrometallurgy, the most ancient technology, remains yet the major extractive process employed by the industry. There are many variants in this process, well documented in modern and classical literature. Because of its high energy consumption, environmental effects and contribution to global warming, pyrometallurgy is becoming less attractive from the point of view of Green Chemistry. In addition, one has to deal with the gradual depletion of the rich ores, since pyrometallurgy requires a high metal content to be economically viable.

Hydrometallurgy, in contrast, is expanding all over the world as a green alternative to pyrometallurgy. It already plays an important role in the production of aluminum, cobalt, copper, gold, molybdenum, nickel, platinum, selenium, silver, tellurium, tungsten, uranium, zirconium, and other metals. Hydrometallurgy is based on the release of metal ions from the ores, by the action of acids, such as H_2SO_4, or bacteria, followed by the formation of complexes with organic reagents and their extraction in organic solvents. The use of solvent extraction, usually referred as SX, is an important step of purification of the metal element. Nowadays, hydro-metallurgy is particularly employed for the so-called oxidized ores, such as metal oxides and carbonates, exhibiting a lower metal content. In contrast, metal sulfide ores are preferred in pyrometallurgy, because of their higher metal content. However, this aspect is changing gradually, by the development of suitable hydrometallurgy leaching processes for metal sulfide ores, including the use of new bacteria species.[11-15]

Hydrometallurgy is about two centuries old, but it can be considered recent in relation to the millenary pyrometallurgy. In 1763, M. V. Lomonosov proposed some ideas related to hydrometallurgy for extracting metals from ores, but only in 1843 P. R. Bagration reported its application to the metallurgy of gold by the cyanidation process. Industrial use of hydrometallugy in the extraction of copper has only started at the beginning of the 20th century.[5] Nowadays, hydrometallurgy is employed in the production of high purity metals and is growing rapidly, stimulated by the green aspects associated with the use of room temperature processes and a more rational engineering, enabling the recovery of the chemical reagents and solvents.[7-24] However, hydrometallurgy still uses huge amounts of organic solvents and intensive chemical processing to perform the extraction of the metal ions after their complexation with organic reagents. A large variety of extractors has been employed, all displaying very large dimensions, placed horizontally as tanks or as vertical columns. However, the intensive manipulation of solvents and extraction processes departs from the currently accepted green principles.

Another important process, coupled with the pyrometallurgy and hydrometallurgy extraction, consists in the electrochemical deposition of the metal. This process is known as electrowinning (EW), and is employed when high purity metals are desired. In industrial processes, it involves large electrodes, high metal ion concentrations and demand several days for performing efficient electrodeposition of the element.[5]

This article will not deal with the classical pyrometallurgical and hydrometallurgical processes, since the subject is already well consolidated in the literature.[3-7] Instead, a new emerging technology will be discussed. It incorporates the recent advances in nanotechnology, by exploring the use of functionalized superparamagnetic nanoparticles for capturing, transporting, concentrating and promoting the electrochemical deposition of metals, under sustainable conditions. This process has been denoted magnetic nanohydrometallurgy, MNHM.[25]

2. Superparamagnetic nanoparticles in magnetic nanohydrometallurgy

Mineral technology is a very common topic in the literature, but mineral nanotechnology is surprisingly scarce, exposing the current lack of nanotechnological developments in extractive metallurgy. The existing comments related to mineral nanotechnology actually refer to the effects of decreasing the size of the ores in the metallurgical process, an aspect that is not advantageous because of the marginal problems involved. Sometimes, mineral nanotechnology is associated with the exploitation of the nano- and microstructures found in biominerals.

In the conventional mineral technology, hydrometallurgy has been performed using complexing agents to capture metal ions from aqueous solutions and transfer them to the organic phase. A typical example is the organic chelating agent shown in (1), employed in copper extraction.

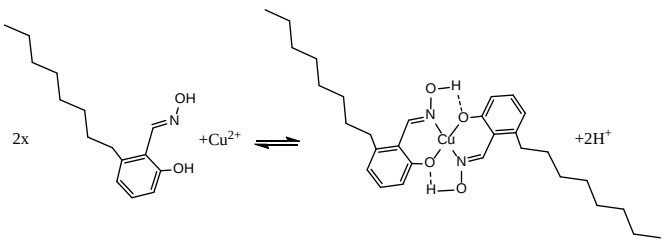

(1)

The organic phase is usually composed by compounds such as tributylphosphate or di-2-ethylhexylphosphate dissolved in kerosine.

In order to understand the advantages of using superparamagnetic magnetite nanoparticles in hydrometallurgy, a detailed explanation is necessary, encompassing: 1) their structural and magnetic properties, 2) the role of the chemical protection and functionalization and 3) their outstanding electrochemical behaviour under magnetically confined conditions.

2.1 Structural and magnetic properties of magnetite nanoparticles

Magnetite is a mixed valence iron oxide material of Fe_3O_4 or formally $Fe^{II}0.Fe^{III}{}_2O_3$ composition, displaying an inverted spinel structure, in which the Fe^{II} ions are located in octahedral sites (O_h) , and the Fe^{III} ions are located both in octahedral (O_h) and tetrahedral (T_d) sites. In this particular structural arrangement, which can be represented as $[Fe^{3+}(\uparrow)]_{Td}[Fe^{3+}(\downarrow)Fe^{2+}(\uparrow)]_{Oh}$, the spin vectors of the Fe^{III} sites are coupled antiferromagnetically, cancelling out their contribution to the resulting magnetic moment. In contrast, the Fe^{II} sites do not exhibit this effect, responding for the strong magnetization behaviour in a magnetic field [26]

The magnetic response of a material in the presence of an applied magnetic field H_o, is given, in cgs units, by

$$B = H_o + 4\pi M \quad (2)$$

where M is the intrinsic magnetization, associated with the atomic contribution, expressed by

$$M = \chi H_o d \quad (3)$$

involving the magnetic susceptibility term, χ, and density, d. The magnetic susceptibility χ is related to the magnetic moment μ by

$$\mu = (3k \chi T/N^2)^{1/2} \quad (4)$$

expressed in terms of a magnetic unity called Bohr Magneton (0.927 x 10^{-20} erg $Gauss^{-1}$)

The global magnetization involves the sum of all magnetic moments, and follows an inverse dependence with the temperature, as expressed by Curie's law or Curie-Weiss Law. At the nanoscale, the individual magnetic moments of the Fe_3O_4 nanoparticles orient rapidly in the applied magnetic field, yielding a global magnetization which tends to a saturation behaviour, as shown in Fig. 1.

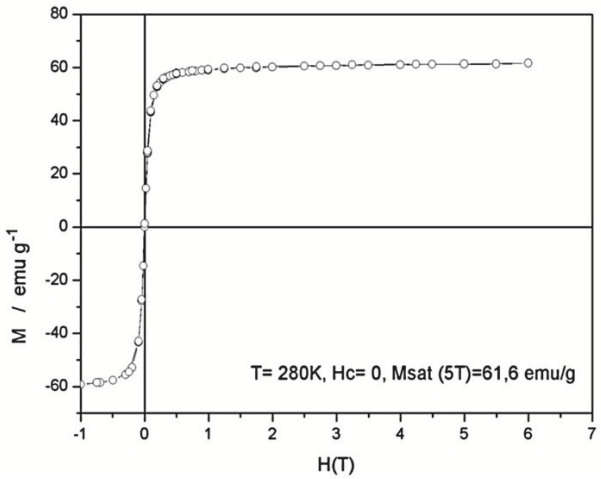

Fig. 1 Magnetization curve for MagNP@ oleic acid at 280 K, illustrating the superparamagnetic behaviour, with no hysteresis.

At the saturation point, practically all the nanoparticle magnetic dipoles are oriented in the same way, or in parallel, exhibiting a maximum magnetization value. In the case of pure magnetite, this value is 92 $Am^2 kg^{-1}$ (or 92 emu g^{-1} in cgs unit). For magnetite nanoparticles coated with an organic layer of oleic acid, the saturation magnetization becomes 62 emu g^{-1}, reflecting the presence of the non magnetic organic material,[27] as shown in Fig. 1. In this example, at room temperature, the magnetization curve remained identical after reversing the scanning of the magnetic fields. This response is typical of superparamagnetic nanoparticles, indicating that the magnetization responds simultaneously to the changes in the magnetic field. At low temperatures, e.g. 8 K, some of the orientation of the magnetic moments can persist during the scanning of the applied magnetic fields. In this case, an incongruence of magnetization curves can be detected, as shown in Fig. 2 (inset), indicating the occurrence of hysteresis.[28]

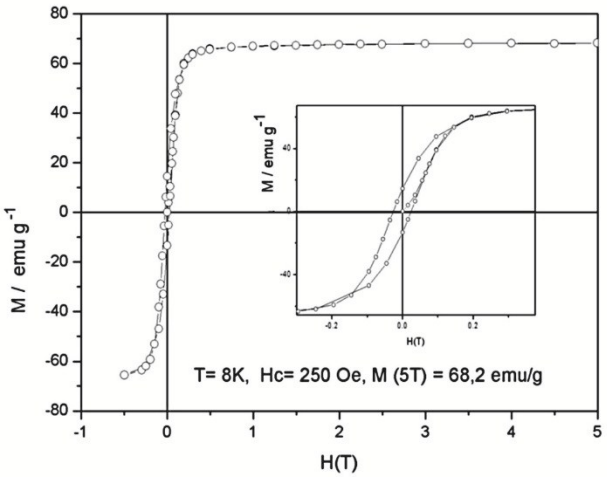

Fig. 2 Magnetization curve for MagNP@oleic acid at 8 K showing the occurrence of a small hysteresis (inset).

A similar behaviour can be observed as the size of the magnetic nanoparticles increases, due to the occurrence of multiple magnetic domains. By monitoring the magnetization response at an specific applied field, as a function of the temperature, it is possible to evaluate the blocking temperature of the material, as shown in Fig. 3. In this case, one can start from a zero field cooling (ZFC), where the magnetic moments are randomly distributed, and then rise the temperature in the presence of a magnetic field. As the temperature increases, the magnetic moments start to orient in the magnetic field increasing the magnetization response. The temperature at which a maximum magnetization is attained represents the blocking temperature. On the other hand, if the sample is cooled in the presence of the magnetic field, the orientation of the magnetic dipoles at the blocking temperature is preserved, generating a characteristic plateau in the magnetization curve. This procedure is called field cooling (FC), and the maximum magnetization response depends on the magnitude of the applied field.[28]

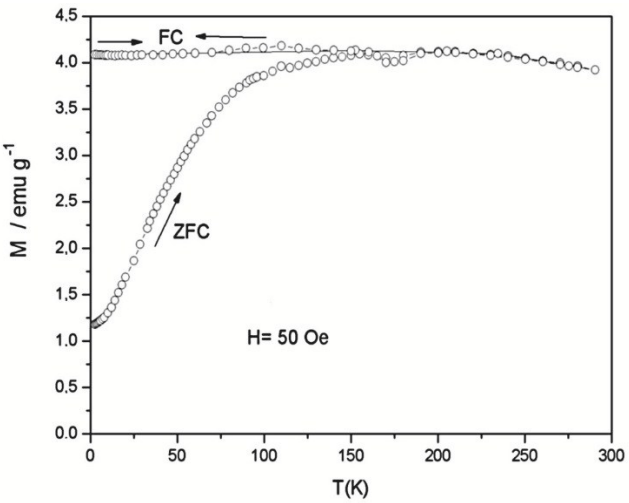

Fig. 3 Field cooling (FC) and zero field cooling (ZFC) curves for MagNP@oleic acid at an applied field of 50 Oe.

In spite of being an abundant magnetic mineral, magnetite is obtained in the industry by synthetic routes, usually aiming the production of black iron oxide pigments. For this type of application, their magnetic properties are not particularly relevant. However, in magnetic nanohydrometallurgy, a strong magnetization response is an important aspect to be pursued. There are many synthetic procedures for generating superparamagnetic nanoparticles, as already reported in the literature.[27,29]

A general method is based on the coprecipitation of Fe(II) and Fe(III) hydroxides, mixed under stoichiometric proportions, at strongly alkaline solutions and controlled heating, stirring rates and atmosphere.

$$Fe^{2+} + 2Fe^{3+} + 8OH^- \rightarrow Fe_3O_4 + 4H_2O \quad (5)$$

The coprecipitation method is quite simple and efficient, and leads to highly magnetic nanoparticles, but spanning a relatively large distribution of sizes, depending on the experimental conditions. The precipitated superparamagnetic material can be easily confined and processed, using commercially available external magnetics, such as those based on $Nd_2Fe_{14}B$, exhibiting 11 kOe of magnetic field.

Under acidic conditions and in the presence of air, the Fe(II) ions at the surface are oxidized to Fe(III), and the structural reorganization promotes the migration of ions generating internal vacancies, leading to a magnetic oxide called maghemite, or γ-Fe_2O_3. In contrast to the black colour of magnetite, the oxidized maghemite material exhibits a brown colour and a better thermal resistance, in spite of its smaller magnetization values (72 emu g^{-1}). Maghemite can be prepared by many different methods,[30-33] but it is also associated with the natural ageing of the magnetite nanoparticles, noted when exposed to the atmosphere and solvents by the gradual change of colour from black to brown.

Another rather simple method consists in the controlled oxidation of iron(II) salts, e.g. $FeSO_4$, by heating in strongly alkaline solutions, in the presence of air, or preferentially in the presence of stoichiometric amounts of $NaNO_3$ under vigorous stirring. The reactions involve the formation of $Fe(OH)_2$ and $Fe(OH)_3$ species, but the role of the nitrate ions seems quite unusual. In this process, the formation of NH_3 can be easily perceived from its characteristic smell, supporting the occurrence of reaction (6) in parallel with the oxidation with O_2 (7).

$$12Fe^{2+} + 23OH^- + NO_3^- \rightarrow 4Fe_3O_4 + NH_3 + 10H_2O \quad (6)$$

$$6Fe^{2+} + 3O_2 + 4OH^- \rightarrow 2Fe_3O_4 + 2H_2O \quad (7)$$

This method leads to large nanoparticles, displaying strong magnetic response.

From the point of view of Green Chemistry, the reported methods should be preferred, since they are carried out in aqueous media, and the separation and isolation processes can be readily performed with an external magnet, with no need of employing filtration or centrifugation steps. Organic solvents are not involved, and the reaction is essentially quantitative, leaving only sodium sulfate or chloride as environmentally acceptable contaminants. The main product, magnetite, is quite abundant in nature, and offers no risk of manipulation, storage or disposal.

Another important method, is based on the thermodecomposition of metal organic compounds, such as those derived from acetilacetonates, nitrosofenilhydroxylamines, metal-carbonyls and fatty acids. The heating is performed by refluxing in high boiling point solvents, such as octadecene, n-eicosane and tetracosane in the presence of surfactants, under high temperatures, vigorous stirring and inert atmosphere. The process requires the careful control of all variables, but usually leads to a narrow distribution of nanoparticles size, stabilized with a lipophilic shell of the organic acid or surfactants.[34-41]

Hydrothermal processes have also been successfully employed in the preparation of superparamagnetic nanoparticles. Typical applied pressures and temperatures are around 2000 psi and 200 ^oC respectively, and variables, such as solvent, concentration and time should be carefully controlled.[42-48] There are also many other methods of preparation of superparamagnetic nanoparticles,[49-55] including those based on the use of surfactants and micelles. Such methods explore the reactions in the confined media promoted by the micelles, and are susceptible to a large number of variables, such as the surfactants composition and concentration, temperature, electrolytes and solvents.

2.2 Chemical protection and functionalization

In aqueous solution the superparamagnetic nanoparticles are exposed to the acid-base reactions with the solvent and the chemical species dissolved, including the redox reactions with molecular oxygen. On the other hand, it is important to keep the nanoparticles as stable suspensions, by preventing or slowing down the formation of precipitates or large agglomerates.

Nanoparticles stabilization depends on the forces acting at the surface level, as described by the DLVO (Derjaguin, Landau, Verwey, Overbeek) theory.[56] There are four types of forces, of van der Waals, electrostatic, magnetic or dipolar, and steric nature involving the nanoparticles surface. Their control depend on the nanoparticles nature, charges and the chemical species anchored at the surface. The best way to perform this task is by modifying the particles with appropriate functional groups, capable of increasing the electrostatic and steric repulsion and prevent agglomeration.

For long term applications, it is also important to protect the magnetite nanoparticles surface, and a simple way is by applying a silica coating, using for instance tetraethoxysilane, $(C_2H_5O)_4Si$, based on the Stöber method.[57] The silica coated magnetic nanoparticles can be represented by $MagNP@SiO_2$. The silica shell obtained by this method exhibits many Si- OH groups at the surface, facilitating further silanization reactions with functionalized organosilanes (Fig. 4). The amounts of silanes employed should be small, just enough to provide a thin protective coating, in order to prevent the formation of silica aggregates. The silanization process is particularly convenient in terms of Green Chemistry, since it is essentially quantitative, proceeds at room temperature, and yields only ethanol in addition to the coated nanoparticles.

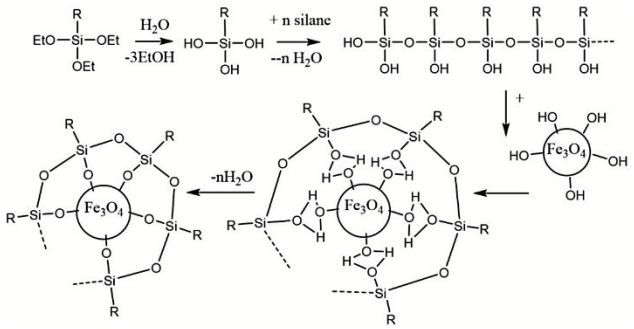

Fig. 4 Silanization scheme starting with the partial hydrolysis and polymerization of the ethoxysilane, followed by the binding and coating of the superparamagnetic nanoparticle. When R is an ethoxy group, a silica coating is obtained, and another silanization process can be applied in order to introduce a suitable functional group.

Direct modification of the superparamagnetic nanoparticles is also possible using catecholate agents, polymers and metal nanoparticles, specially for application in catalysis.[58] For applications in magnetic nanohydrometallurgy, the organosilanes should introduce functional groups capable of binding metal ions, such as amines and polyamines, imidazole, thiols, carboxylates, phenols and catechols, oxymes, and thiocarbamates. Alternatively, the functional groups can also act as coupling agents, in order to bind specific ligands, such as EDTA.[59-63] This procedure has also been successfully employed for the immobilization of enzymes on superparamagnetic nanoparticles.[64-69] A very common organosilane species is the aminopropyl-triethoxysilane, APTS. It is employed in the generation of the functionalized nanoparticle, MagNP@SiO_2/APTS[27] or MagNP@SiO_2/Si(pr)(NH_2). In the last representation Si(pr)(NH_2) represents the silanepropylamine coating. Again, the silanization should involve small amounts of organosilanes, producing only ethanol in addition to the functionalized nanoparticles.

The binding of metal ions to such immobilized ligands follows the basic principles of coordination chemistry, and depends on the pH, temperature and interfering agents. The chemistry involved is rather well known, and this is a great advantage of dealing with this type of system. The most important aspect, however, is the possibility of sequestering metal ions for transporting and concentrating them at a specific surface, with the aid of a magnetic field or a simple miniature magnet. By applying the basic strategies of coordination chemistry, it is possible to release the metal ions, and to perform selective reactions at the nanoparticles surface, for catalytic or analytical purposes.

Another interesting material successfully tested for application in MNHM is based on carbon powder modified with superparamagnetic nanoparticles. As a matter of fact, carbon materials, such as carbon black, pyrolytic carbon, glassy carbon and graphite, provide effective interfaces in electrochemical processes,[70-71] and in the micro/nanoparticulate form, they exhibit very large surface areas for application in adsorption and separation processes.[72-76]

The binding of the magnetic nanoparticles on carbon materials is facilitated by the use of a lipophilic coating, such as oleic and stearic acids. For this reason, the synthetic procedures based on the thermodecomposition methods are suitable for this purposes, specially those obtained with oleic acid.[39] The MagNPs generated in this process are stabilized by an oleic acid coating, facilitating their attachment to the carbon surface. A typical example is illustrated by the SEM image in Fig. 5. This material was obtained as a black suspension after mixing the MagNPs with carbon powder (Aldrich, Darco® G60), in toluene, at 1:9 MagNp:carbon mass ratio. This material was denoted as Cmag.

After sonicating, the suspension can be separated by using an external magnet and washed with water. The final adsorbing material is essentially composed by carbon particles containing for instance 0.16 g (6.9 x 10^{-4} mol) of Fe_3O_4 per gram of Cmag. In this case, the surface area and total pore volumes, measured by N_2 adsorption/desorption analysis were 572 $m^2\ g^{-1}$ and 0.473 $cm^3\ g^{-1}$, respectively, in comparison to 713 $m^2\ g^{-1}$ and 0.606 $cm^3\ g^{-1}$, for the original activated carbon, measured under similar conditions.[70,71] Therefore, the incorporation of the magnetic nanoparticles does not preclude adsorption processes at carbon, leading just to a small decrease, around 20%, in the surface area and porosity of the carbon material. This aspect is more than compensated by the possibility of collecting and concentrating the carbon material at electrodes, in order to perform their magnetically confined electrochemistry under preconcentration conditions

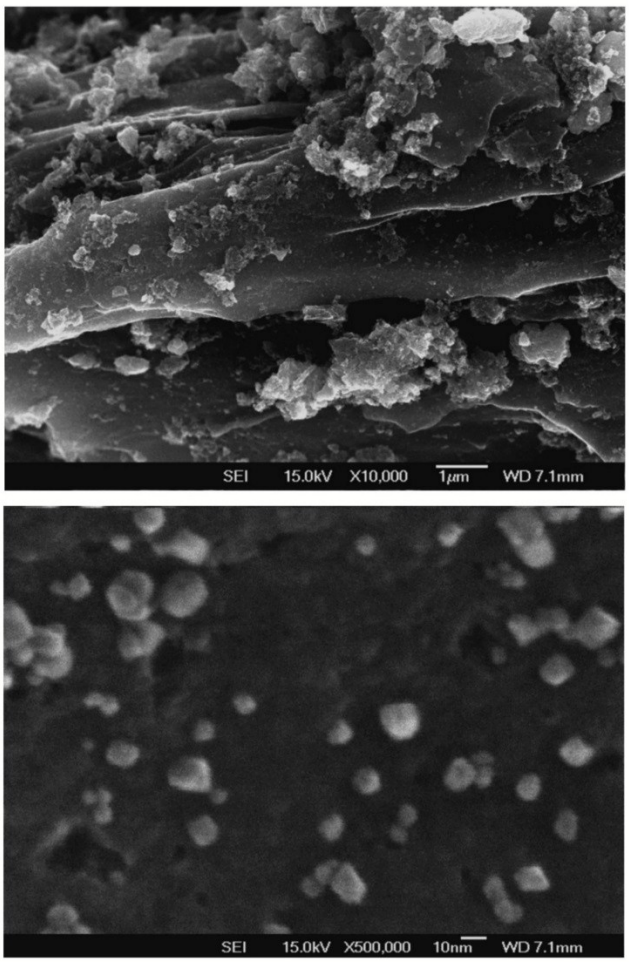

Fig. 5 SEM image of (CMag) carbon modified with MagNP@oleic acid, at a 9:1 proportion (top) and its expanded view showing the anchored magnetic nanoparticles (bottom).

2.3. Electrochemical behaviour under magnetically confined conditions

A third, and perhaps most relevant aspect for hydrometallurgy applications, is the electrochemical behaviour of the superparamagnetic nanoparticles, magnetically confined at the electrode surface.[77]

When a magnet is placed externally at the electrode, the randomly suspended superparamagnetic nanoparticles in solution are rapidly attracted, covering completely its exposed surface. Under this condition, the electrochemically active species are not able to reach the electrode surface, and the magnetic nanoparticles form a blocking layer, precluding any significant electrochemical process.

However, when redox active species including the metal ions, are directly attached to the nanoparticles, the electrochemical conduction becomes feasible by electron hopping and ion transport mechanisms, generating very strong signals, because of their preconcentration at the electrode surface. This outstanding behaviour allows to explore the electrochemistry of nanoparticles magnetically confined at the electrode, in association with the nanohydrometallurgy process, leading to a new process called magnetic nanohydrometallugy.

The first evidence of electron transport through the magnetically confined nanoparticles was obtained[78] by attaching the complex aquapentacyanidoferrate(II) to the available amino groups from MagNP@SiO_2/APTS, as illustrated in scheme (8).

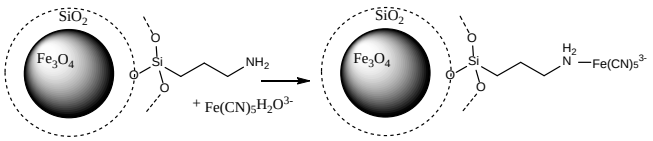

(8)

The covalent coating of the MagNP@SiO_2/APTS particles with the aminopentacyanidoferrate(II) ions, yields MagNP@SiO_2/APTS-$Fe(CN)_5^{3-}$, exhibiting enhanced electrochemical signals associated with the Fe(III)/(II) redox couple, in relation to those observed for the same complex solutions, in the absence of the magnetic nanoparticles (Fig. 6).

The parent hexacyanidoferrate(II) ions, are not able to bind to MagNP@SiO_2/OSiprNH$_2$ because of their kinetically inert character, and do not exhibit its characteristic electrochemical response (Fig. 7).

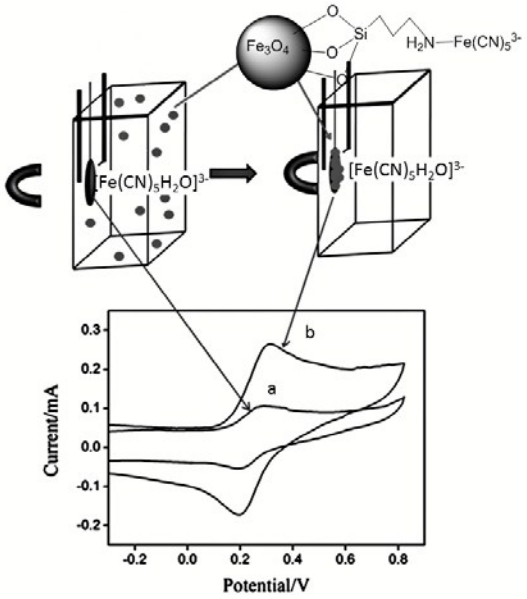

Fig. 6. Cyclic voltammetry of $[Fe(CN)_5H_2O]^{3-}$ (5.0×10^{-5} mol L^{-1}) in aqueous solution containing KNO_3 (0.10 mol L^{-1}), and an equivalent amount of MagNP@APTS-$Fe(CN)_5^{3-}$, platinum electrode, scan rate = 100 mV s^{-1} (a) in the absence and (b) in the presence of the external magnet (E *vs* Ag/AgCl). Reprinted with permission from ref. 73.

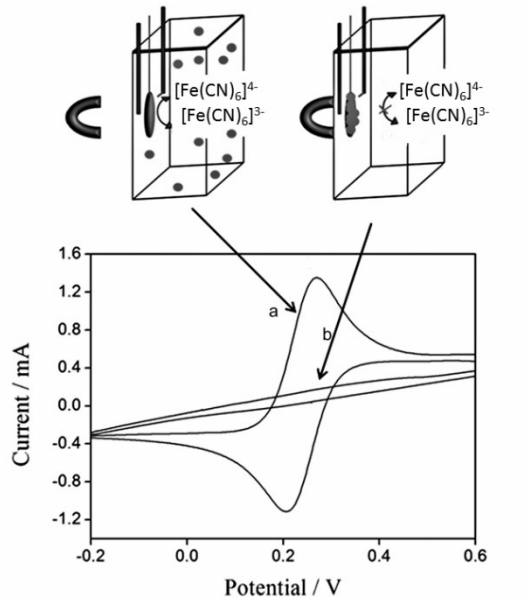

Fig. 7. Blocking experiment using MagNP@SiO_2/APTS, showing the cyclic voltammetry (10 mV s^{-1}) response of $[Fe(CN)_6]^{4-}$ ions (1.0×10^{-3} mol L^{-1}) in 0.10 mol L^{-1} KNO_3 aqueous solution, a) before and b) after applying the external magnet (E vs Ag/AgCl). Reprinted with permission from ref. 73.

3. Magnetic Nanohydrometallurgy of Copper

Copper(II) ions form stable complexes with a large variety of ligands, and a typical example is ethylenediamine, $NH_2CH_2CH_2NH_2$. This classical ligand acts as a chelating species, and there is a commercially available ethylenediaminepropyltriethoxysilane agent suitable for direct application on the superparamagnetic nanoparticles.

In order to understand the reactions involved in the capture of copper(II) ions, it is interesting to compare the stability constants of the related 3d metal complexes with ethylenediamine, as shown in Fig. 8. The illustrated trend in this Figure is known as the Irving-Williams series. It reflects the contribution of the ligand field stabilization energies and the Jahn-Teller effect on the stability constants along the series of metal ions. As indicated in the Figure, copper(II) ions form the most stable 1:1 and 1:2 complexes in the series. In this case, the binding of the third ligand is precluded by the Jahn Teller effect, but the weakening of the axial bonds, is compensated by the strengthening of the equatorial bonds, thus increasing K_1 and K_2.

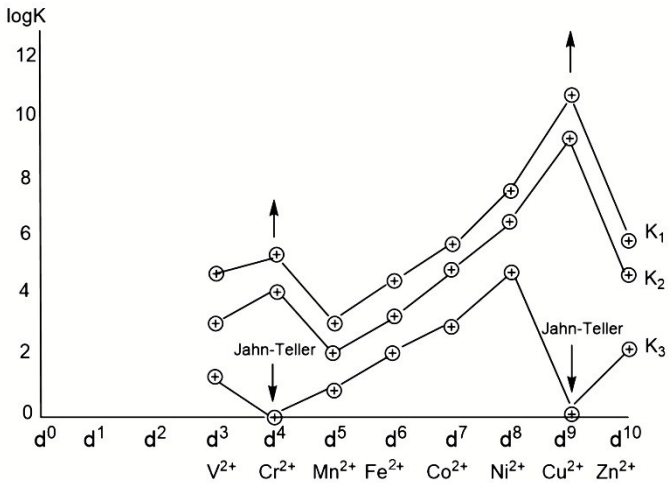

Fig. 8 Variation of the stability constants K_1, K_2 and K_3 of ethylenediamine complexes of 3d transition elements.

As a matter of fact, copper ions are easily captured by superparamagnetic nanoparticles treated with ethylediaminepropyltriethoxysilane,[25] or EnPTS (scheme 9).

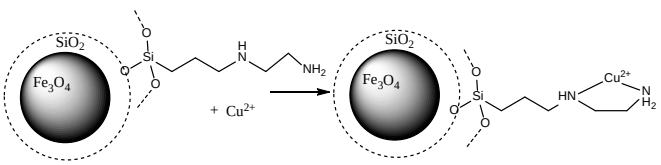

This process was initially developed for electroanalytical applications, in order to improve the detection of copper ions by means of the magnetic preconcentration effects at the electrode surface, as illustrated in Fig. 9.

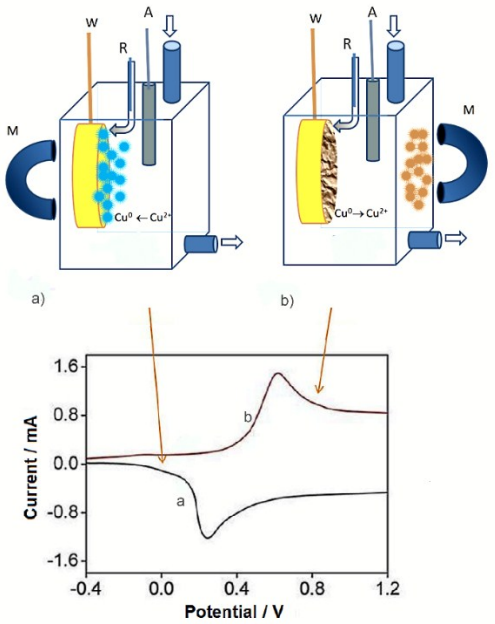

Fig. 9 Electrochemical cell (W = gold working electrode, R = reference electrode (Ag/AgCl), A = platinum auxiliary electrode, M = magnet), and square wave voltammograms (150 mV s^{-1}) of MagNP/EnPTS (a) magnetically confined at the gold disc electrode after their interaction with Cu^{2+} ions (2.0 x 10^{-3} mol L^{-1}) and (b) the corresponding reverse stripping analysis, confirming the electrodeposition of the metal. Reprinted with permission from ref. 25.

In the absence of the magnetic nanoparticles, the observed electrochemical signal from the copper(II) deposition at the bare electrode is very small, or practically negligible. After the magnetic confinement, the electric currents become very strong, indicating the electrochemical deposition of the captured copper(II) ions. By reversing the potential, a stripping current can be observed, consistent with the electrodissolution of the metallic copper films.

The superparamagnetic nanoparticles coated with the copper(II) complexes species behaved as a redox conducting layer, allowing efficient electron transfer to the electrode. The observed voltammograms exhibited a profile coherent with a diffusion controlled behaviour for a nanoparticle film, thicker than the diffusion length of the electroactive species. The kinetic regime was similar to that observed for the modified electrodes coated with a layer dendrimeric particles encompassing a large number of ferrocenyl groups.[79-80] The capture of copper ions from the solution and their association with the superparamagnetic nanoparticles, has been confirmed by energy dispersed X-Ray (EDX) analysis as shown in Fig. 10.

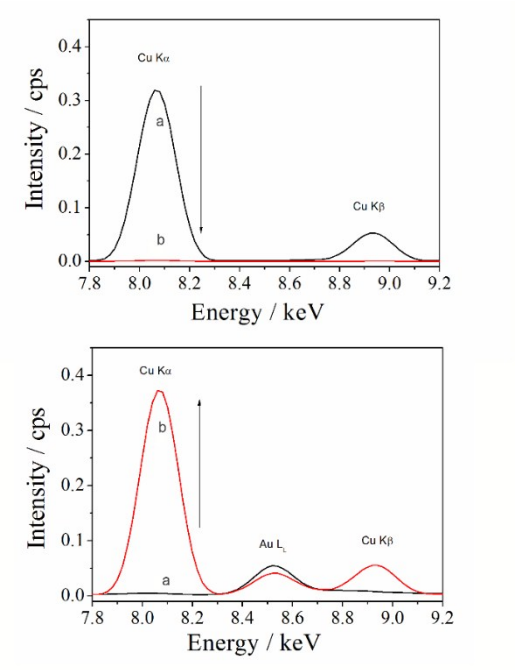

Fig. 10 EDX analysis of copper(II) containing MagNP/EnPTS, after removing from the electrolyte solutions (top) and of the gold electrode surface (bottom) before (a) and after performing de magnetic confined electrolysis (b). Reprinted with permission from ref. 25.

It should be noted that the capture, transport, concentration and electrodeposition of copper proceed in single step, with high efficiency. The conventional use of polluting solvents and extraction processes is being completely eliminated. In addition, the functionalized nanoparticles are completely recyclable, returning to the process after the electrodeposition step. These are important advantages to account in terms of Green Chemistry

Interference from competing metal ions is a general problem in coordination chemistry, and cannot be neglected in hydrometallurgy. Fortunately, because of the rather distinct stability constants (Fig. 8), a good metal ion selectivity can be achieved by controlling the pH and exploring the competitive reactions of protons in the coordination process, as expressed by eq. (10) and (11).

$$\text{MagNP@SiO}_2\text{/EnPTS} + 2H^+ \rightleftharpoons \text{MagNP@SiO}_2\text{/(EnH}_2^+\text{)PTS} \quad (10)$$

$$\text{MagNP@SiO}_2\text{/EnPTS} + M^{2+} \rightleftharpoons \text{MagNP@SiO}_2\text{/(MEn}^{2+}\text{)PTS} \quad (11)$$

The stability constants of Mn^{2+}, Fe^{2+}, Co^{2+} and Zn^{2} complexes with ethylenediamine are at least 5 orders of magnitude smaller in comparison with the Cu^{2+} complex (Fig. 8). By decreasing the pH their reactions can be completely inhibited, eliminating their possible interference in the hydrometallurgical process. Such interference can also be controlled at the end of the process, by adjusting the applied voltage in order to promote the stepwise selective deposition of the metal ions, such as Ag(I) or Pb(II), without conflicting with the electrodeposition of copper. This strategy has already been demonstrated in the eletroanalytical determination of copper in the MNHM process.[25]

For electrometallurgical purposes, it is necessary to optimize the capture of the copper ions, which is limited by the number of complexing groups available at the nanoparticles surface. This point depends upon the functionalization process and nanoparticles size. As already mentioned, the interference from metal ions, pH and complexing agents should be carefully controlled. Therefore, each process should be optimized, based on the composition of the substrates and the reactor design. Ancillary complexing agents can also be added, as part of the coordination chemistry strategy, to improve the capture of the element or to mask eventual interferences from the existing metal ions in solution.

As a proof of concept, the magnetic hydrometallurgy process has been applied to the recovery of copper ions from 0.020 mol L^{-1} concentrated solutions, as shown in Fig. 11. In this experiment, the amount of active MagNP@SiO_2/EnPTS was kept relativey small, in order to explore the efficiency of the successive cycling. The capture and electrodeposition of copper monitored by the EDX technique and cyclic voltammetry, confirmed the viability of the method in the laboratory scale.[25]

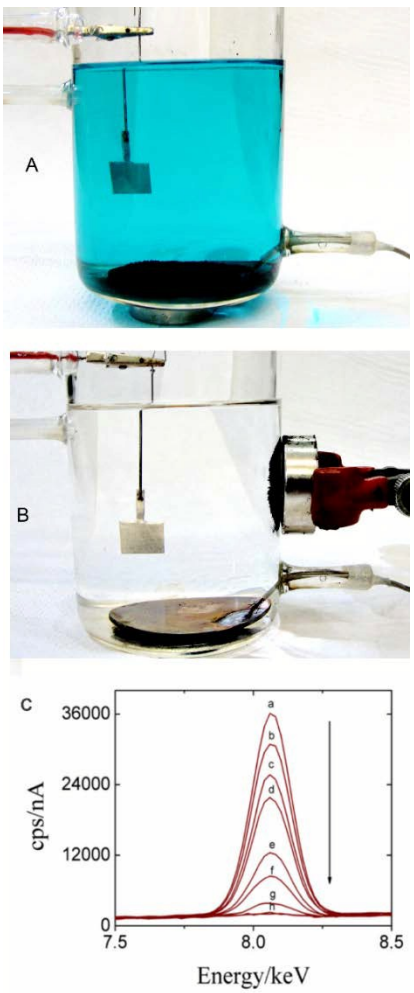

Fig. 11. Starting Cu^{2+} solution (20 x 10^{-3} mol L^{-1}) with the MagNP@SiO_2/EnPTS magnetically confined at the copper electrode at the bottom (A), and after 7 successive capture/electrolytical cycles (B), as monitored by EDX, (C) showing the gradual decay (a-g) and the depletion (h) of the metal ions from the solution. Reprinted with permission from ref. 25.

An automated process has already been designed to demonstrate the possibility of conducting the NHM process under programmable conditions, using relatively small equipment and facilities (Fig. 12). In the tested experimental setup, the applied potentials, stirring, magnet positioning and draining functions were computer controlled, allowing to run the complete sequence of metal capture, confinement and electrodeposition in the same reactor, in a continuous way.

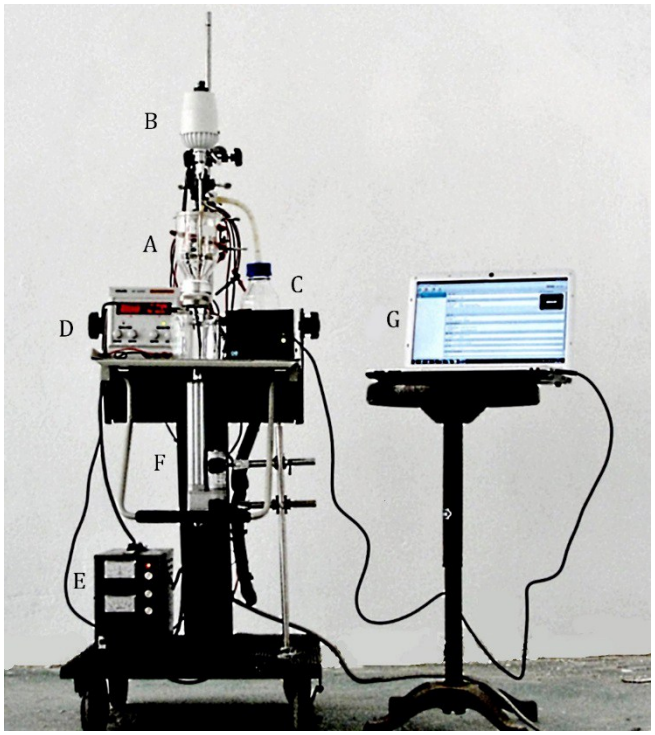

Fig. 12 Automated setup for a computer controlled NHM process, including the reaction flask (A), stirrer (B), pump (C), power sources (D, E), magnet assembly (F) and controller (G).

4. Magnetic hydrometallurgy of Silver

Silver is an important element found in copper mines. It often occurs in the presence of gold. It has been traditionally used as a noble material in houseware and jewellery, and is particularly remarkable for exhibiting the highest electrical and thermal conductivity of all metals. Its great economical relevance reflects the increasing technological applications, including the use in antibacterial products.[81-82] However, nowadays, its presence as a contaminant species in the environment is also increasing, because of the accumulation of electronic wastes.[83] For this reason, there is an intrinsic economical and environmental interest of exploring the recovery of silver[84-86] under sustainable conditions.

For capturing and processing silver ions using the NHM process it is possible to use many distinct nanoparticles, such as those functionalized with thiols, because of the great compatibility between the Ag^+ and R-SH species. In a recent paper, carbon powder incorporating superparamagnetic nanoparticles, Cmag, has been successfully tested in the nanohydrometallurgy of silver.[72] As a matter of fact, carbon, from many different sources, has already been employed for adsorbing metal ions[81] including gold and silver from gold-plant solutions.[60]

In contrast with the complexing agents, the capture of silver by the carbons surfaces is based on adsorption. It can be easily monitored by EDX. The adsorbed mass of silver ions at equilibrium concentration q_e (mg g^{-1}) can be expressed by eq. 12, where C_0 and C_e (mg L^{-1}) are the initial and equilibrium concentrations, respectively, V (L) is the volume of solution used for the adsorption assay, and m (g) is the mass of dry Cmag.

$$q_e = \frac{(C_0 - C_e)\,V}{m} \qquad (12)$$

An isotherm can be generated from the adsorption capacities *versus* equilibrium concentrations, as expressed by the Langmuir equation,[72] which in the linearized form becomes (13)

$$\frac{C_e}{q_e} = \frac{1}{Q_{max}\,K_L} + \frac{C_e}{Q_{max}} \qquad (13)$$

where C_e (mg L^{-1}) is the equilibrium concentration of silver ions in solution, q_e (mg g^{-1}) is the value of the adsorbed silver ions at equilibrium, Q_{max} (mg g^{-1}) and K_L (L mg^{-1}) are constants related to the adsorption capacity and energy of adsorption, respectively. The feasibility of using Cmag on the adsorption of silver ions can be evaluated from the values of the separation factor (R_L), according to eq. 14, where C_0 (mg L^{-1}) is the initial concentration of silver ion. If $R_L > 1.0$ the process is considered unfavorable, and $0 < R_L < 1$ the process is favorable.

$$R_L = \frac{1}{(1 + C_0 K_L)} \qquad (14)$$

Another formalism is based on the Freundlich isotherm, which encompasses a reversible process and includes the formation of multilayers, as well as a variety of adsorption sites and nature of the adsorbed species. The logarithmic form of the Freundlich isotherm is expressed by eq. 15, where k_F indicates the adsorption capacity and n reflects the intensity of adsorption.

$$\log q_e = \log k_F + \frac{1}{n}\log C_e \qquad (15)$$

A typical adsorption isotherm of silver ions onto Cmag at 298K can be seen in Fig. 13.A. From the linearization of the adsorption isotherm, it is possible to determine the adsorption capacity of Cmag for Ag^+ ions. In this example, the Langmuir model provided a better fit for the data obtained for the adsorption of silver ions on Cmag, leading to a value of 61.5 mg/g for the adsorptive capacity at 298 K (Fig.13.B). The values of R_L between 0.10 and 0.48, indicated the viability of using Cmag for the removal of silver ions.[64] In comparison with the results reported for activated carbon[62], the efficiencies are rather similar, in spite of the slight decrease of the surface area by the coating of magnetic nanoparticles.

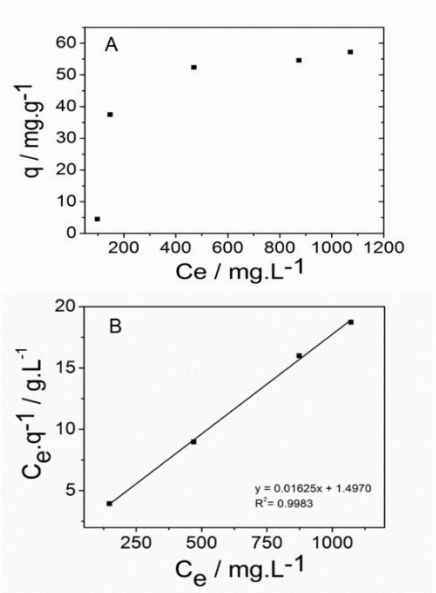

Fig. 13. (A) Adsorption isotherm of Cmag in Ag^+ solutions at 298 K, and (B) the corresponding linearization by the Langmuir model. Reprinted with permission from ref. 72.

Carbon materials are widely employed in electrodes, even in the particulate form, as in the case of carbon paste electrodes. For instance, in order to evaluate the electrochemical behaviour of Cmag, 50 mg of the powder was suspended in 100 mL of $AgNO_3$ (0.1 mol L^{-1}) under stirring, for 1 h. A large excess was employed in order to saturate the carbon material with silver ions. After this step, the powder was concentrated with a magnet, washed with water, and 2 mg was transferred to the electrochemical cell containing 3 mL of the electrolyte solution. The square wave voltammograms of the magnetically confined Cmag/Ag^+ particles are shown in Fig. 14. For comparison purposes, a voltammogram of the starting Cmag material, not previously exposed to the silver ions, can also be seen in Fig. 14.

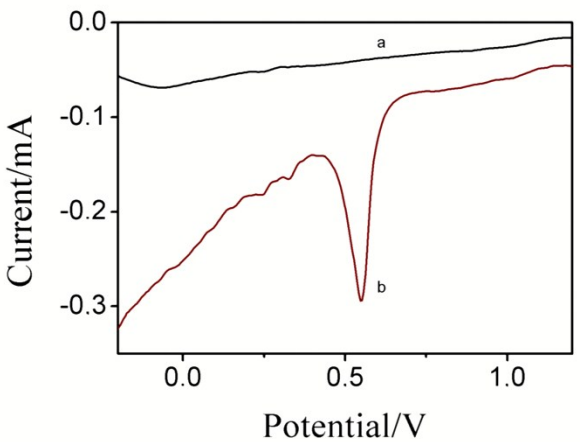

Fig.14. Square wave voltammograms of (a) the starting Cmag material magnetically confined at the electrode, in the presence of the electrolyte solution (1.10^{-2} mol.L^{-1} of KNO_3) and (b) of Cmag, after saturating with Ag^+ ions, showing the Ag^+ reduction peak at 0.51 V. Reprinted with permission from ref. 72.

Impedance measurements have been carried out for the Cmag electrodes, in comparison with the bare gold electrode. The impedance spectrum of the gold electrode was essentially diffusional, exhibiting a typical charge-transfer resistance R_{CT}= 20 Ohm, Rs = 20 Ohm, C_{dl} = $1.5x10^{-6}$ F, W = $3.8x10^{-3}$ in equivalent circuit. In the case of the superparamagnetic carbon electrode, at high frequencies, a kinetic regime consistent with a charge-transfer resistance R_{ct} = 70 Ohm (R_s = 20 Ohm, C_{dl}= 2.1 $x10^{-6}$ F, W = 4.4 $x10^{-3}$) was observed, while at low frequencies, the diffusional regime predominated. Therefore, the magnetic carbon electrode has a slightly lower conductivity than gold, reflecting the multiple interfaces involving the magneticaly assembled particles. However, it is interesting to notice that a comparative experiment carried out under similar conditions with a bare glassy carbon electrode, led to a charge transfer resistance of 380 Ohm. Surprisingly, the superparamagnetic carbon electrode has a better performance than the traditional glassy carbon electrode.

Ionic migration has been demonstrated by the detection of the silver deposit formed at the electrode surface. In order to confirm this, after the electrodeposition step, the electrode was removed from the solution, washed with water, acetone and dried. The EDX spectra of the electrode, before and after the electrochemical process, (Fig. 16) exhibited the peaks at 22.2 and 25 keV, associated with the kα and kβ lines of silver, corroborating the electrodeposition of the element at the electrode surface.

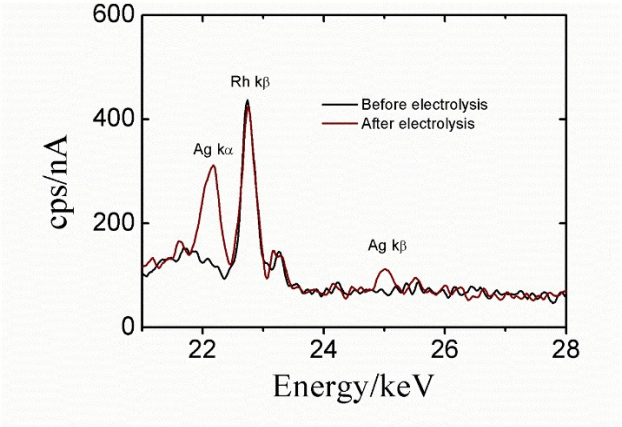

Fig. 15. EDX spectra of the electrode, showing the signals of the Rh lamp and of the silver element, before and after the electrolysis. Reprinted with permission from ref. 72.

In addition, a similar EDX analysis was carried out for Cmag. Starting from the Ag^+ saturated Cmag material, and submitting to a magnetically confined electrodeposition at the electrode, at -0.2 V for 5 min., there was a 60 % signal decay of the silver ions from the carbon particles. By repeating the process, the second analysis led to the complete depletion of silver ions from the Cmag film, indicating their transference to the metallic electrode.

The silver recovery from photographic plates has been performed, by cutting the films into small pieces and treating with concentrated nitric acid. After neutralizing the nitric extract with sodium hydroxide, the resulting solution was transferred to an automated reactor as illustrated in Fig. 12, and treated with 500 mg of Cmag under stirring, during 5 min. In the sequence, the external

magnet was positioned at the back of the electrode and after 2 min. the Ag^{+}/Cmag coated electrode was submitted to -0.5 V for 3 min. At this point, the process was interrupted for a sampling procedure by recording the EDX spectra. This process allowed the complete recovery of silver metal from the solution.[72]

5. Magnetic hydrometallurgy of Mercury

Mercury and its common chemical forms are toxic, persistent species in the environment, exhibiting a great tendency to accumulate in biota.[87-88] It is a contaminant species in many natural resources, including mines and petroleum, and their exploitation has been a critical source of pollution and environmental problems. In spite of its prohibition, mercury is yet illegally employed in the extraction of gold from open mines and rivers, contaminating the environment and aquatic life, while poisoning the population by the ingestion of contaminated fishes. Mercury is accumulative in the body, interacting strongly with biomolecules, specially at the sulfur atoms from aminoacids and proteins.

Therefore, the removal of mercury from the mineral resources and petroleum represents a great challenge to pursue in a sustainable world. The advantage of using MNHM in this case is the facility of forming complexes with mercury ions, and their easy electrodeposition and recycling, from aqueous and non aqueous media.

The environmental impact of mercury is a complex subject, because the element is present in many different forms, including the elementary species, and their inorganic salts ($HgCl_2$, $HgCl(aq)^{+}$, Hg_2Cl_2), oxides and organometallic compounds ($[Hg(CH_3)_2]$, $[Hg(CH_3)Cl]$). Fortunately, because of the high affinity of mercury for sulfur ligands, such species will react with thiol complexing agents. Therefore, their immobilization on the superparamagnetic nanoparticles provides an efficient way of collecting the element, even at highly diluted conditions, allowing its removal, confinement and recovery.

The first attempt to demonstrate the possibility of using MNHM in the detection and removal of mercury ions from water and petroleum, was based on their reaction with the superparamagnetic nanoparticle functionalized with mercaptopropyltriethoxisylane (MPTS) as in scheme (16):[76]

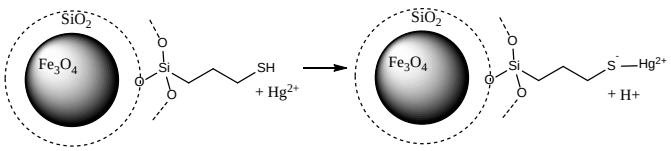

(16)

Typical voltammograms of the MagNP@SiO_2/MPTS nanoparticles after their reaction with Hg^{2+} ions can be seen in Fig. 16.

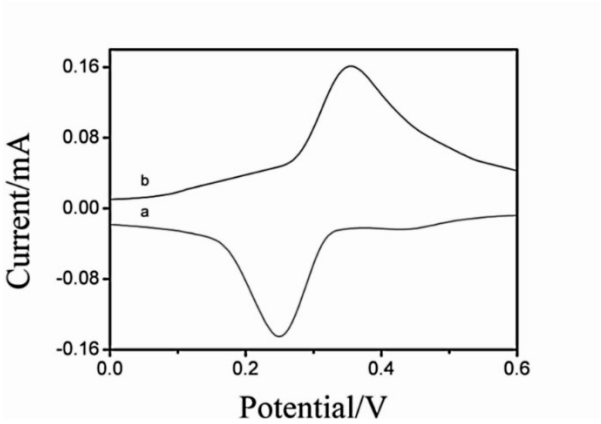

Fig. 16 Square wave voltammogram showing in cathodic scan (a), the reduction of Hg^{2+} ions coordinated to the superparamagnetic nanoparticles, and in the anodic scan (b) the metal stripping, after removing the superparamagnetic nanoparticles from the working electrode surface; Scan rate=150 mV s^{-1} ; KNO_3 1.0 x10^{-1} mol L^{-1} was used as electrolyte (pH 7). Reprinted with permission from ref. 71.

The cathodic scan reflects the electrochemistry of the mercury ions coordinated to the sulfur groups of MPTS, and in the absence of the superparamagnetic nanoparticles, this wave is very small. The cathodic wave is strongly enhanced by the magnetically induced pre-concentration of the Hg-MPTS-MagNPs onto the electrode surface, with the integrated current peaks consistent with the expected amount of mercury ions in the samples.

After the cathodic scan, the superparamagnetic nanoparticles can be removed from the working electrode surface, and a reverse anodic scan can be applied, as shown in Fig. 16. In this case, a rather strong wave was also observed around 0.35 V, indicating a stripping condition, where most of the mercury atoms were already deposited onto the electrode surface. It should be noted that even in this case, the stripping condition is greatly improved in relation to the conventional procedure, since the deposition can be performed in a single step with the aid of the superparamagnetic nanoparticles, with no need of performing exhaustive electrolysis. This is a relevant green aspect, reducing the number of processing steps and improving the yield.

When the superparamagnetic nanoparticles containing mercury ions were removed from the solutions and analysed for the metal content using Energy Dispersive X-ray fluorescence (EDX) measurements the results were quite consistent with those obtained electrochemically.

The nanoparticles were highly effective not only for capturing mercury ions from aqueous solution and in crude oil samples, but also for concentrating them at the electrode surface with the aid of an external magnet. Their good electrochemical response allowed to perform *in situ* electrochemical analysis, with no need to dissolve then in order to release the mercury ions (Fig. 17.A) as in the conventional analytical methods.

For the capture of mercury from oil, typically, the samples can be diluted with n-hexane and the MagNP/MPTS particles added. After sonicating for 30 min, the superparamagnetic nanoparticles can be collected with a magnet, and washed sequentially with n-hexane, acetone and water, before transferring into the electrochemical cell. In the reported example,[76] the current response measured under magnetically confined conditions varied linearly with respect to the concentrations of $HgCl_2$, , is shown in Fig.17.B.

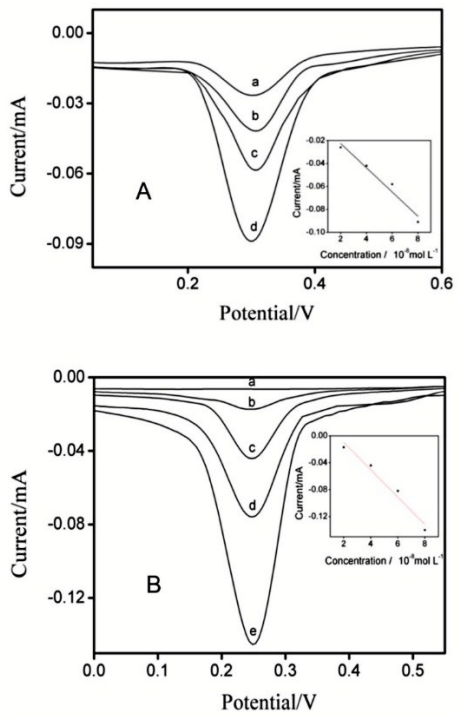

Fig. 17 (A) Square wave voltammograms of magnetically confined MagNP@SiO_2/MPTS nanoparticles treated with 10 ml of aqueous solutions containing a) 2 x 10^{-8}, 4 x 10^{-8}, 6 x10^{-8}, 8 x 10^{-8} mol L^{-1} Hg^{2+} ions, or (B) after collecting following from crude oil samples containing (a-e) 0 to 8 x 10^{-8} mol L^{-1} mercury ions. (F= 30 Hz , E_{step} = 0.005 V, E_{Time} = 10 s Scan rate=150 mV s^{-1} , 0.6V→-0.4V ; KNO_3 1.0.10^{-1} mol L^{-1} was used as electrolyte (pH 7) Reprinted with permission from ref. 71.

Interference studies involving metal ions, as well as pH dependence, are quite relevant in coordination chemistry processes, and has been investigated by performing the experiments in the presence of buffers or typical contaminants such as Pb^{2+}, Ni^{2+} and Cu^{2+} ions. The best sensitivity has been obtained in the pH 7 to 9 range, corresponding to the pKa of the thiol groups. Above pH 10, mercury ions tend to precipitate as oxo-hydroxo compounds, while below pH 6 there is a competition between the H^+(aq) and Hg^{2+} ions for the thiolate sites. Metal ions interference depends on their affinity for the thiol groups, and in this sense, the great advantage of the mercury ions is quite well known. In addition, the interference can also be discriminated by the selected deposition potentials of the metal ions involved. Interference studies were carried out at the same pH employed for the eletroanalytical detection of mercury ions, under no influence of precipitation reactions usually observed above pH 9. The electrochemical response of the captured mercury ions at 0.3 V was not influenced by the presence of Pb^{2+}, Cu^{2+} and Ni^{2+} ions, even though a small signal for Pb^{2+} can be observed at -0.4 V.

The capture and electrodeposition of mercury ions has also been performed using carbon modified with superparamagnetic nanoparticles. Typical square wave voltammograms of the magnetically confined particles previously treated with 2 x 10^{-6} - 4 x 10^{-3} mol L^{-1} Hg^{2+} ions can be seen in Fig. 18. There is a sharp enhancement of the signals, due to the high local concentration of the Hg^{2+} ions, exhibiting a good linearity with the concentration of the mercury ions.

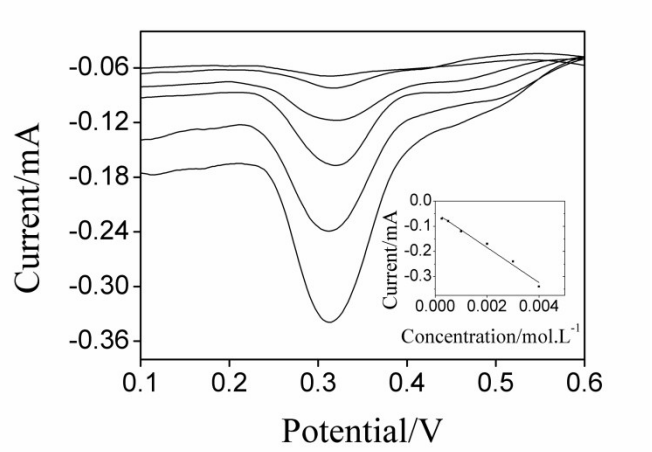

Fig. 18 Square wave voltammograms of superparamagnetic carbon electrode, in the presence Hg^{2+} ions in the range of 2 x 10^{-6} - 4 x 10^{-3} mol L^{-1}, using an external magnet, frequency = 30 Hz, amplitude 50 mV, E step = 5 mV, KNO_3 0.5 mol L^{-1}. Reprinted with permission from ref. 72.

The voltammetric response for Pb^{2+} ions has only been observed at the 10^{-3} mol L^{-1} range, as shown in Fig. 19. Even in this case, there is a pronounced deviation from linearity below 2x10^{-3} mol L^{-1}, indicating a much smaller affinity for the magnetic carbon substrate, as compared with the mercury ions. It has been shown that Cu^{2+} and Ni^{2+} ions are not interferents in the detection of Pb^{2+} and Hg^{2+} ions.

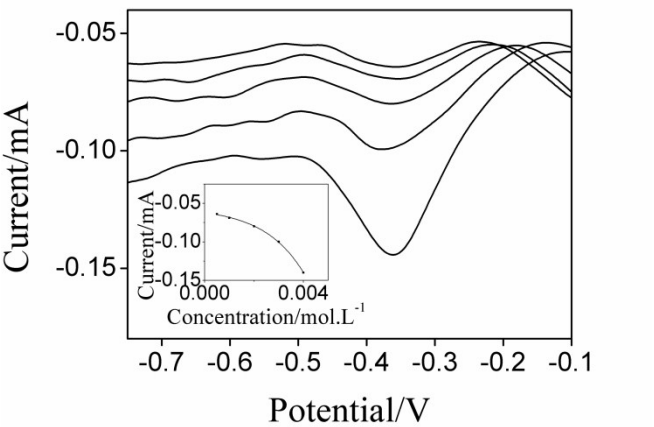

Fig. 19 Square wave voltammograms of superparamagnetic carbon electrode, in the presence of an external magnet, frequency = 30 Hz, amplitude 50 mV, E_{step} = 5 mV, for Pb^{2+} ions in the range of 0.5 = 4 x10^{-3} mol L^{-1} . Reprinted with permission from ref. 72.

Conclusions and Final Remarks

A recent publication has focused on the advantages of the nanotechnology and green chemistry partnership, highlighting the possibilities of improving efficiency and quality of processes, achieving a better economy of energy and materials, promoting

catalysis under mild conditions and facilitating the online monitoring of production lines and environment.[89] As a matter of fact, nanoparticles and nanomaterials are being increasingly explored in green chemistry applications, as reflected in the recent publications in the literature, including this journal.[58]

In this regard, magnetic nanohydrometallurgy represents an important technological innovation, matching practically all the basic principles of green chemistry. While exploring the same principles of coordination chemistry successfully applied in modern extractive hydrometallurgy process, it encompasses a distinct nanotechnological appeal, using specially designed superparamagnetic nanoparticles for capturing, transporting, confining and processing metal ions, with the aid of an external magnet.

The superparamagnetic nanoparticles are based on magnetite, a very common mineral exhibiting practically no toxic effects, and all the procedures are carried out in aqueous media, using commercially available reagents.

The working nanoparticles are completely recoverable after the electrodeposition process, sustaining a cyclic process which can be automated, without using organic solvents and intensive chemical processing, as required in the conventional extractive hydrometallurgy and electrowinning processes.

The electrodeposition process is magnetically concentrated at the electrode, allowing to explore the preconcentration effect and improving the electrochemical performance in relation to the conventional process.

At the laboratory scale, the entire procedure can be performed in the same reactor, minimizing the number of processing steps.

Magnetic separation and recycling can be easily carried out, just by using an external, commercial magnet. This means a rather straigthford and clean process, in relation to conventional precipitation, filtration or solvent extraction processes.

All these aspects associated with magnetic nanohydrometallurgy contemplate the basic green chemistry recommendations in terms of simplicity, economy of steps, materials and energy, use of environmentally compatible reagents, including the aqueous media, recycling of the materials, improving efficiency of the processes, with low toxicity involved. More than improving a green metallurgical process, it can also be applied in environmental problems, by removing hazardous metal ions, and processing them.

Finally, it should be mentioned that important initiatives are being conducted all over the world, to improve metal lixiviation with the aid of biotechnology. This can be indeed a great progress, since the use of bacteria accelerates the process, and proceeds under mild conditions. Biolixiviation is also allowing to extract metal ions from low content ores and residues which are accumulating in the mines, yielding relatively diluted solutions which are stored in tanks or lakes for further processing. MNHM can advantageously couple with the biolixiviation process, starting from its very end point, and leading to the pure metal. Such partnership provides a holistic insight of a totally green hydrometallurgical process for the production of metals under sustainable conditions.

Acknowledgements

The support from Fundação de Amparo à Pesquisa Científica e Tecnologica do Estado de Sao Paulo, FAPESP – Grant 2013/24725-4, and Conselho Nacional de Desenvolvimento Científico e Tecnológico, CNPq, Grant 482383/2013-5 is gratefully acknowledged.

References

1. J. H. Clark. *Green Chem*. 2006, **8**, 17-21.
2. J. F. Jenck, F. Agterberg, M. J. Droescher. *Green Chem. 2004*, **6**, 544-556.
3. F. Habashi, *Principles of Extractive Metallurgy*, vols. 1-2, Gordon & Breach, NewYork-London-Paris, 1970,
4. K. N. Han, *Metallurgical and Materials Trans*. 2003, **34B**, 757-767.
5. W. G. Davenport, M. King, M Schlesinger and A. K, Biswas, *Extrative metallurgy of copper*, Elsevier, Oxford, 4th Ed., 2002.
6. J. C. Painter, *J. South African Institute Mining Metallurgy, 1973*, 158-169.
7. K. Rotuska and T. Chmielewski, *Physicochemical Problems of Mineral Processing, 2008*, **42**, 29-36.
8. H. Brandl, Microbial leaching of metals. In: H. J. Rehm (ed), Biotechnology, Vol. 10, Wiley-VCH, Weinheim, 2001, pp. 191-224.
9. H. R. Watling, *Hydrometallurgy*, *2014*, **146**, 96-110.
10. H. R. Watling, D. M. Collinson, J. Li, L. A. Mutch, F. A. Perrot, S. M. Rea, F. Reith, E. L. J. Watkin, *Minerals Engineering*, *2014*, **56**, 35-44.
11. G. J. Olson, J. A. Brierley, C. L. Brierley, *Applied Microbiol. Biotechnol*., *2003*, **63,** 249-57.
12. T. Rohwerder, T. Gehrke, K. Kinzler and W. Sand, *Applied Microbiol. Biotechnol. 2003*, **63**, 239-48.
13. M. Maley, W. van Bronswijk, H. R. Watling, *Hydrometallurgy*, *2009*, **98**, 66-72.
14. H. R. Watling, *Hydrometallurgy*, *2008*, **91**, 70-88.
15. H. R. Watling, *Hydrometallurgy*, *2006*, **84**, 81-108.
16. J. Petersen. *Hydrometallurgy*, *2010*, **104**, 404 –409.
17. H. M. Veit, A. M. Bernardes, J. Z. Ferreira, J. A. S. Tenorio, C. D. Malfatti. *J. Hazard. Mater*., 2006, **137**, 1704-1709
18. K. Scott, X. Chen, J. W. Atkinson, M. Todd, R. D. Armstrong. *Resour. Conserv. Recycl*.**,** 1997**, 20**, 43-55.
19. L. R. Gouvea, C. A. Morais. *Miner. Eng***.,** *2010***,** **23**, 492-497
20. F. Habashi. *J. Min. Metallurgy*. 2009, **45**, 1-13.
21. P. Fornari, C. Abbruzzese. *Hydrometallurgy, 1999*, **52**, 209-222.
22. F. A. Lemos, L. G. S. Sobral, A. J. B. Dutra. *Miner. Eng. 2006*, **19**, 388-398.
23. A. J. B. Dutra, G. P. Rocha, F. R. Pombo. *J. Hazard. Mater*., *2008*, **152**, 648-655.
24. B. Panda, S. C. Das. *Hydrometallurgy , 2001*, **59**, 55-67.
25. U. Condomitti, A. Zuin, A. T. Silveira, K. Araki, H. E. Toma. *Hydrometallurgy 2012*, **125**, 148-151.
26. C. Kittel. *Phys. Rev.*, 1946, **70,** 965-971.

27. M. Yamaura, R. L. Camilo, L. C. Sampaio, M. A. Macedo, M. Nakamura and H. E. Toma, *J. Magn. Magn. Mat.*, *2004*, **279**, 210-217.
28. B. D. Cullity, Introduction to Magnetic Materials, Addison-Wesley, Reading, MA., 1972.
29. S. Laurent, D. Forge, M. Port, A. Roch, C. Robic, L. V. Elst and R. N. Muller, *Chem. Rev.*, *2008*, **108**, 2064-2110.
30. R. Massart and V. Cabuil, *J. Chimie Physique et Physico-Chimie Biologique*, *1987*, **84**, 967-973.
31. N. Fauconnier, A. Bee, J. Roger and J. N. Pons, *Prog. Colloid Polym. Sci.*, *1996*, **100**, 212-216.
32. N. Fauconnier, A. Bee, J. Roger and J. N. Pons, *J. Mol. Liq.*, *1999*, **83**, 233-242.
33. N. Fauconnier, J. N. Pons, J. Roger and A. Bee, *J. Colloid Interface Sci. 1997*, **194,** 427-433.
34. J. Rockenberger, E. C. Scher and A. P. Alivisatos, *J. Am. Chem. Soc.*, *1999*, **121**, 11595-11596.
35. D. Farrell, S. A.Majetich and J. P.Wilcoxon, *J. Phys. Chem. B* , *2003*, **107**, 11022-11030.
36. N. R. Jana, Y. Chen and X. Peng, *Chem. Mater.*, *2004*, **16**, 3931-3935.
37. A. C. S. Samia, K. Hyzer, J. A. Schlueter, C.-J. Qin, J. S. Jiang, S. D. Bader and X.-M. Lin, *J. Am. Chem. Soc. 2005*, **127**, 4126-4127.
38. Y. Li, M. Afzaal and P. O'Brien, *J. Mater. Chem. 2006*, **16**, 2175-2180.
39. J. Park, K. An, Y. Hwang, J.-G. Park, H.-J. Noh, J.-Y. Kim, J.-H. Park, N.-M. Hwang, and T. Hyeon, *Nat. Mater. 2004*, **3**, 891-895.
40. S. Sun, H. Zeng, D. B. Robinson, S. Raoux, P. M. Rice, S. X. Wang and G. Li, *J. Am. Chem. Soc.*, *2004*, **126**, 273-279.
41. Y. W. Jun, Y. M. Huh, J. S. Choi, J. H. Lee, H. T. Song, S. Kim, S. Yoon, K. S. Kim, J. S. Shin, J. S. Suh and J. Cheon, *J. Am. Chem. Soc.*, *2005*, **127**, 5732-5733.
42. T. Hyeon, S. S. Lee, J. Park, Y. Chung and H. Bin Na, *J. Am. Chem. Soc.*, *2001*, **123,** 12798-12801.
43. K. Butter, K. Kassapidou, G. J. Vroege and A. P. Philipse, *J. Colloid Interface Sci.*, *2005*, **287**, 485-495.
44. B. Mao, Z. Kang, E. Wang, S. Lian, L. Gao, C. Tian and C. Wang, *Mater. Res. Bull.*, *2006*, **41**, 2226-2231.
45. H. Zhu, D. Yang and L. Zhu, *Surf. Coat. Technol.*, *2007*, **201**, 5870-5874.
46. S. Giri, S. Samanta, S. Maji, S. Ganguli and A. J. Bhaumik, *J. Magn. Magn. Mater*, *2005*, **285**, 296-302.
47. J. Wang, J. Sun, Q. Sun and Q. Chen, *Mater. Res. Bull.*, *2003*, **38**, 1113-1118.
48. S. Lian, Z. Kang, E. Wang, M. Jiang, C. Hu and L. Xu, *Solid State Commun.*, *2003*, **127,** 605-608.
49. K. M. Lee, C. M. Sorensen, K. J. Klabunde and G. C. Hadjipanayis, *IEEE Trans. Magn. 1992*, **28**, 3180-3182.
50. P. A. Dresco, V. S. Zaitsev, R. J. Gambino and B. Chu, *Langmuir*, *1999*, **15**, 1945-1951.
51. C. J. O'Connor, C. Seip, C. Sangregorio, E. Carpenter, S. C. Li, G. Irvin and V. T. John, *Mol. Cryst. Liq. Cryst.*, *1999*, 335, 1135-1154.
52. J. A. Lopez-Perez, M. A. Lopez-Quintela, J. Mira and J. Rivas, *IEEE Trans. Magn.*, *1997*, **33**, 4359-4362.
53. S. Santra, R. Tapec, N. Theodoropoulou, J. Dobson, A. Hebard and W. Tan, *Langmuir*, *2001*, **17**, 2900-2906.
54. M. P. Pileni and N. Duxin, *Chemical Innovation*, *2000*, **30,** 25-33
55. A. H. Lu, E. L Salabas and F. Schueth, Angew. Chem. Int. Ed., 2007, **46**, 1222-1244.
56. E. J. W. Verwey and J. T. Overbeek, *Theory of the Stability of Lyophobic Colloids*, Elsevier, Amsterdan, 1948.
57. W. Stober, A. Fink and E. Bohn, *J. Colloid Interface Sci.*, *1968*, **26**, 62-69.
58. L. M. Rossi, N. J. S. Costa, F. P. Silva and R. Wojcieszak, *Green Chem.*, *2014*, **16**, 2906-2933.
59. F. M. Koehler, M. Rossier, M. Waelle, E. K. Athanassiou, K. L. Ludwig, R. N. Grass, D. Günther and W. J. Stark, *Chem. Comun. 2009*, **32**, 4862-4864.
60. Y. H. Kim, G. Y. Kim and H. B. Lim, Bull. Korean Chem. Soc., *2010*, **31,** 905-909.
61. D. Dupont, W. Brullot, M. Bloemen, T. Verbiest, K. Binnemans, *ACS Appl. Mat. Interfaces*, *2014*, **6**, 4980-4988.
62. D. Dupont, J. Luyten, M. Bloemen, T. Verbiest and K. Binnemans, *Industrial & Engineering Chem. Res.*,*2014*, **53**, 15222-15229.
63. J. Chen, Y. Hao and M. Chen, *Environ. Sci. Pollution Res.*, *2014*, **21,** 1671-1679.
64. C. G. C. M. Netto, L. H. Andrade and H. E. Toma, *Tetrahedron: Asymmetry*, *2009*, **20**, 2299-2304.
65. L. P. Rebelo, C. G. C. M. Netto, H. E. Toma and L. H. Andrade, *J. Braz. Chem. Soc.*, *2010*, **21**, 1537-1542.
66. L. H. Andrade, L. P. Rebelo, C. G. C. M. Netto and H. E. Toma, *J. Mol. Cat. B: Enzymatic*, *2010*, **66**, 55-62.
67. C. G. C. M. Netto, E. H. Nakamatsu, L. E. S. Netto, M. A. Novak, A. Zuin, M. Nakamura, K. Araki and H. E. Toma, *J. Inorg. Biochem.*, *2011*, **105**, 738-744.
68. C. G. C. M. Netto, M. Nakamura, L. H. Andrade and H. E. Toma, *J. Mol. Cat. B: Enzymatic*, *2012*, **84,** 136-143.
69. C. G. C. M. Netto, H. E. Toma and L. H. Andrade, *J. Mol. Cat. B: Enzymatic*, *2013*, **85-86,** 71-92.
70. R. McCreery, *Chemical Reviews*, *2007*, **108**, 2646-2687.
71. I. Svancara, K. Vytras, K. Kalcher, A. Walcarius and J. Wang, *Electroanalytis*, *2009*, **21**, 7-28.
72. C. Moreno-Castilla, M. B. Dawidziuk, F. Carrasco-Marin and E. Morallon, *Carbon*, *2012*, **50**, 3324-3332.
73. R. J. Davidson, V. Veronese and M. V. Nkosi, *J. South African Inst. Mining and Metallurgy*, *1979*, 281-297.
74. R. C. Bansal and M. Goyal, *Activated Carbon Adsorption*, Taylor & Francis, Boca Raton, 2005.
75. A. Omri and M. Benzina, *Desalination and Water Treatment*, *2013*, **51**, 2317-2326.
76. U. Condomitti, A. Zuin, A. T. Silveira, K. Araki and H. E. Toma, *J. Electronal. Chem.*, *2011*, **661**, 72-76..
77. U. Condomitti, A. T. Silveira, G. W. Condomitti, S. H. Toma, K. Araki and H. E. Toma, *Hydrometallurgy*, *2014*, **147-148**, 241-245.
78. U. Condomitti, A. Zuin, M. A. Novak, K. Araki and H. E. Toma, *Electrochem. Comm.*, *2011*, **13**, 72-74.
79. J. D. Qiu, M. Xiong, R. P. Liang, H. P. Peng and F. Liu, *Biosens. Bioelectron.*, *2009*, **24**, 2649-2653.
80. S. Wang, J. M. Noel, D. Zigah, C. Ornelas, C. Lagrost, D. Astruc and P. Hapiot, *Eletrochem. Commun. 2009*, **11**, 1703-1706.
81. C. Levard, E. M. Hotze, G. V. Lowry and G. E. Brown Jr, *Environmental Science & Technology*, *2012*, **46**, 6900-6914.
82. I. K. Sen, A. K. Mandal, S. Chakraborti, B. Dey, R. Chakravorty and S. S. Islam, *Int. J. Biol. Macromol.*, *2013*, **62C**, 439-449.
83. C. Marambio-Jones and E. M. V. Hoek, *J. Nanoparticles Research*, *2010*, **12**, 1531-1551.
84. H. T. Ratte *Environmental Toxicology and Chemistry*, *1999*, **18**, 89-108.
85. A. Modi, K. Shukla, J. Pandya and K. Parmar, I*nt. J. Emerging Technology and Advanced Engineering*, *2012*, **2**, 599-606.

86. J. M. Dias, M. C. M. Alvim-Ferraz, M. F. Almeida, J. Rivera-Utrilla and M. Sanchez-Polo, *J. Environmental Management, 2007*, **85**, 833-846.
87. N. E. Selin, *Ann. Rev. Environ. Resources, 2009*, **34**, 43-63.
88. P. Holmes, K. A. F. James and L. S. Levy, *Science of the total environment, 2009,* **408,** 171-182.
89. H. E. Toma, *Pure Appl. Chem., 2013*, **85**, 1655-1669.

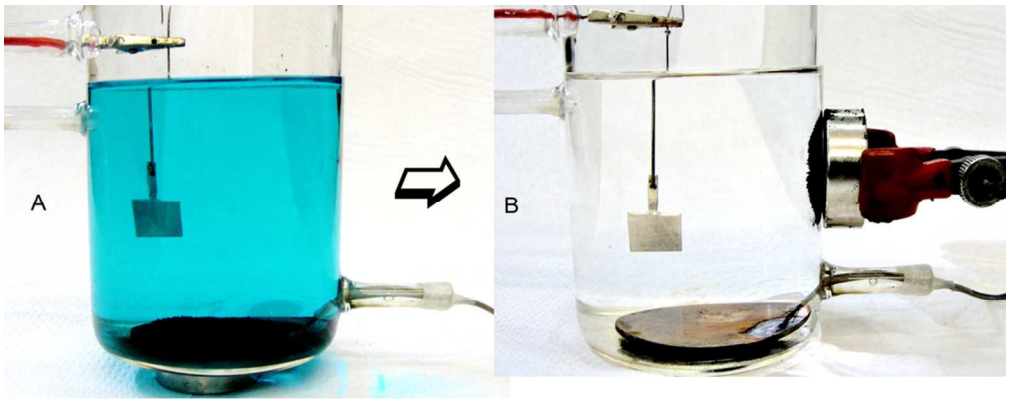

Magnetic nanohydrometallurgy of copper
48x18mm (600 x 600 DPI)